

Impact of nuclear geometry in symmetry plane correlations in OO and Ne–Ne collisions at the LHC

Suraj Prasad

Email: suraj.prasad@wigner.hun-ren.hu

HUN-REN Wigner Research Centre for Physics, Budapest, Hungary

Based on: [arXiv:2605.00866](https://arxiv.org/abs/2605.00866)

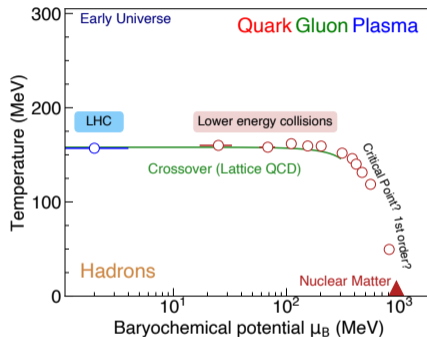
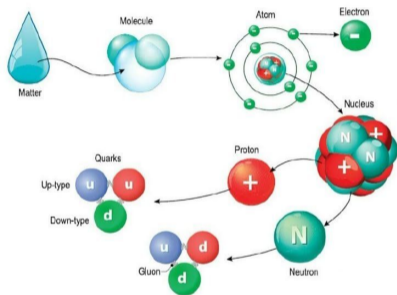
May 28, 2026

GPU Day 2026

- QGP and heavy-ion collision basics
- Anisotropic flow and symmetry-plane correlations
- Nuclear geometry in OO and Ne–Ne collisions
- AMPT model and computing requirements
- SPC results and geometry-driven interpretation
- Summary and outlook

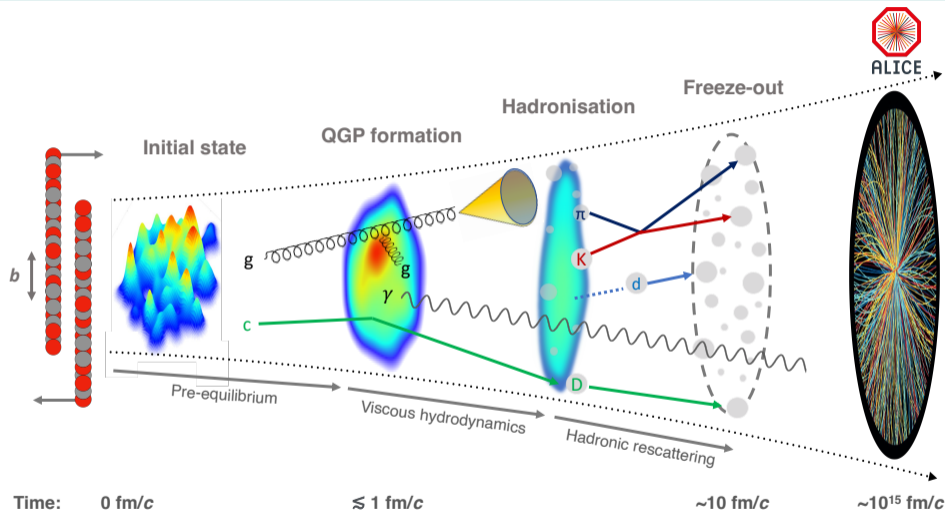
Matter

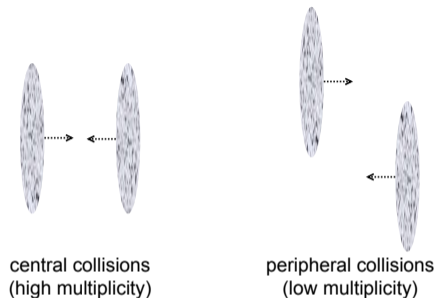
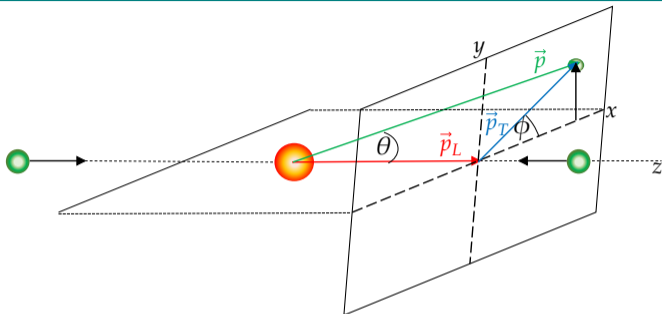
From Molecule to Quarks



ALICE Collaboration, Eur.Phys.J.C 84 (2024), 813

- Quarks/gluons can not exist freely – color confinement
- QGP is a primordial state of matter where the deconfined partons exist freely under thermal equilibrium



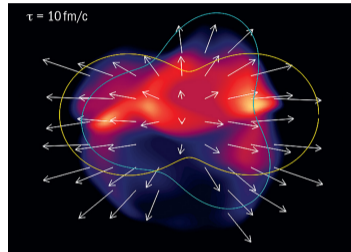
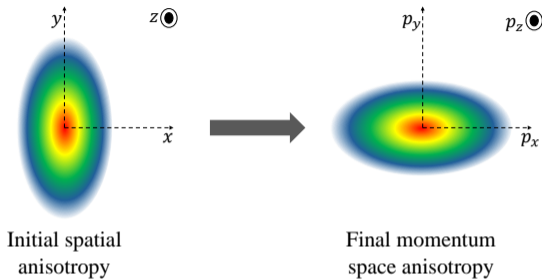


- Transverse momentum (p_T),

$$p_T = \sqrt{p_x^2 + p_y^2};$$
- azimuthal angle (ϕ), $\phi = \tan^{-1}(p_y/p_x)$;

- Polar angle $\theta = \cos^{-1}(p_z/|\vec{p}|)$, where

$$|\vec{p}| = \sqrt{p_x^2 + p_y^2 + p_z^2}.$$
- Pseudorapidity (η), $\eta = -\ln[\tan(\theta/2)]$;
- rapidity (y), $y = \frac{1}{2} \ln \left(\frac{E+p_z}{E-p_z} \right).$

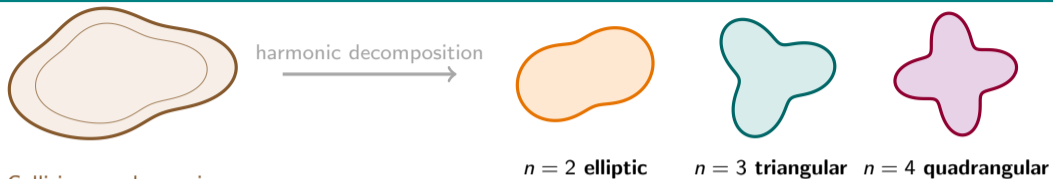


Transformation is driven by collective expansion of QGP leading to observation of final state anisotropic flow coefficients:

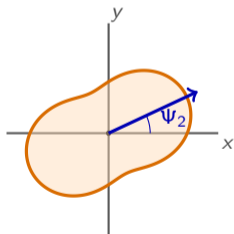
$$\frac{dN}{d\phi} \propto 1 + 2 \sum_{n=1}^{\infty} v_n \cos [n(\phi - \Psi_n)]$$

v_n are the flow coefficients and Ψ_n are the symmetry plane angles. Voloshin and Zhang, Z. Phys. C 70 (1996).

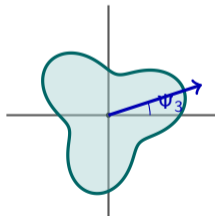
Symmetry Plane Angles (Ψ_n)



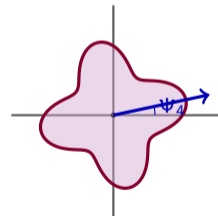
Event-by-event participant fluctuations generate ε_2 , ε_3 , and ε_4 components mapped to v_2 , v_3 , and v_4 .



$n = 2$
elliptic emission



$n = 3$
triangular emission



$n = 4$
quadrangular emission

- Symmetry-plane angles are harmonic-specific orientations of collective flow:

$$\psi_n = \frac{1}{n} \arg(Q_n), \quad Q_n = \sum_{j=1}^M w_j e^{in\phi_j}.$$

- For a large event sample, $\langle \psi_n \rangle \approx 0$.
- **Symmetry Plane Correlations (SPCs)** probe mode coupling beyond single v_n :

$$\text{SPC}(c_1 n_1, c_2 n_2, \dots) = \left\langle \cos \left(\sum_i c_i n_i \psi_{n_i} \right) \right\rangle.$$

- SPCs separate linear response from non-linear hydrodynamic mixing, e.g. $v_4 \leftrightarrow v_2^2$, $v_5 \leftrightarrow v_2 v_3$, etc.
- SPCs are sensitive to initial geometry and transport properties of the QGP, providing stringent tests for theoretical models

The mixed-harmonic correlator can be expressed as Bhalerao, Luzum and Ollitrault, Phys. Rev. C 84 (2011)

$$v_{n_1}^{a_1} v_{n_2}^{a_2} \dots v_{n_k}^{a_k} e^{i(a_1 n_1 \Psi_{n_1} + \dots + a_k n_k \Psi_{n_k})} = \left\langle e^{i(n_1 \phi_1 + n_2 \phi_2 + \dots + n_l \phi_l)} \right\rangle.$$

Under the factorization assumption, the Gaussian estimator used for SPCs is Bilandzic, Lesch and Taghavi, Phys. Rev. C 102 (2020); ALICE, Eur. Phys. J. C 83 (2023)

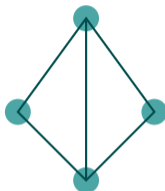
$$\left\langle \cos \left(\sum_i a_i n_i \Psi_{n_i} \right) \right\rangle_{\text{GE}} = \frac{\sqrt{\frac{\pi}{4}} \left\langle \prod_i v_{n_i}^{a_i} \cos \left(\sum_i a_i n_i \Psi_{n_i} \right) \right\rangle}{\sqrt{\left\langle \prod_i v_{n_i}^{2a_i} \right\rangle}}.$$

For the two observables discussed here,

$$\langle \cos [4(\Psi_2 - \Psi_4)] \rangle_{\text{GE}} = \frac{\sqrt{\frac{\pi}{4}} \langle v_2^2 v_4 \cos [4(\Psi_2 - \Psi_4)] \rangle}{\sqrt{\langle v_2^4 v_4^2 \rangle}},$$

$$\langle \cos [6(\Psi_3 - \Psi_6)] \rangle_{\text{GE}} = \frac{\sqrt{\frac{\pi}{4}} \langle v_3^2 v_6 \cos [6(\Psi_3 - \Psi_6)] \rangle}{\sqrt{\langle v_3^4 v_6^2 \rangle}}.$$

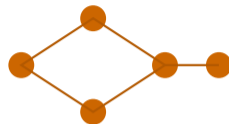
^{16}O : tetrahedral / octupole-rich



projected $4\text{-}\alpha$ tetrahedral motif

- Stronger intrinsic triangular/octupole component.
- Favors larger v_3 -driven nonlinear response.
- Hence larger $\langle \cos[6(\Psi_3 - \Psi_6)] \rangle_{\text{GE}}$ in OO .

^{20}Ne : elongated / quadrupole-rich



elongated "pinball" / $^{16}\text{O} + \alpha$ -like motif

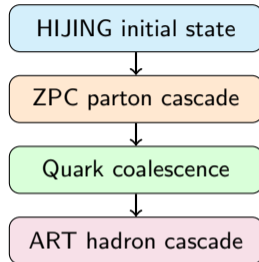
- Stronger intrinsic elliptic/quadrupole deformation.
- Enhances the coupling $v_4 \sim \chi_{4,22}(v_2)^2$.
- Hence larger $\langle \cos[4(\Psi_2 - \Psi_4)] \rangle_{\text{GE}}$ in Ne-Ne .

Prasad and Sahoo, arXiv:2605.00866 (2026); Teaney and Yan, Phys. Rev. C 90 (2014); Gardim et al., Phys. Rev. C 85 (2012).

AMPT string-melting workflow

- 1 HIJING initial state: minijets, strings, geometry.
- 2 ZPC parton cascade: repeated parton scatterings.
- 3 Hadronization by quark coalescence.
- 4 ART hadron cascade until freeze-out.

- One event can produce **dozens to thousands** of final hadrons.
- Transport dominates runtime because each parton/hadron may rescatter multiple times.
- Cost rises with multiplicity, density, and the number of tracked scatterings in both cascades.



- The effects of nuclear geometry are prominent in central collisions
- Dense central events are computationally costly because both N_p and rescattering counts increase

Lin et al., Phys. Rev. C 72 (2005); Zhang et al., Phys. Rev. C 61 (2000); Wang and Gyulassy, Phys. Rev. D 44 (1991); Zhang, Comput. Phys. Commun. 109 (1998); Greco, Ko and Levai, Phys. Rev. Lett. 90 (2003); Li et al., Int. J. Mod. Phys. E 10 (2001).

- For event multiplicity M , naive k -particle correlators scale as

$$\mathcal{O}(M^k) \text{ per event.}$$

- With N_{evt} events and N_{comb} harmonic combinations:

$$\text{Cost}_{\text{naive}} \sim N_{\text{evt}} N_{\text{comb}} M^k.$$

- Q-vector / recursive cumulant methods reduce this to approximately

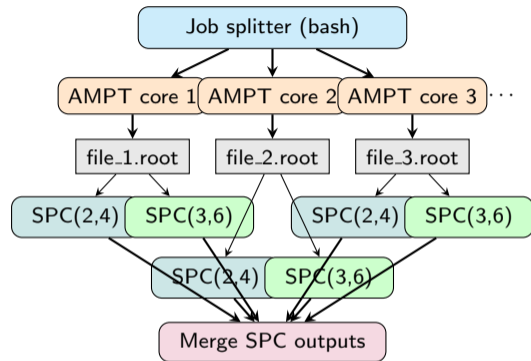
$$\text{Cost}_{\text{Q-vector}} \sim N_{\text{evt}} N_{\text{comb}} k M,$$

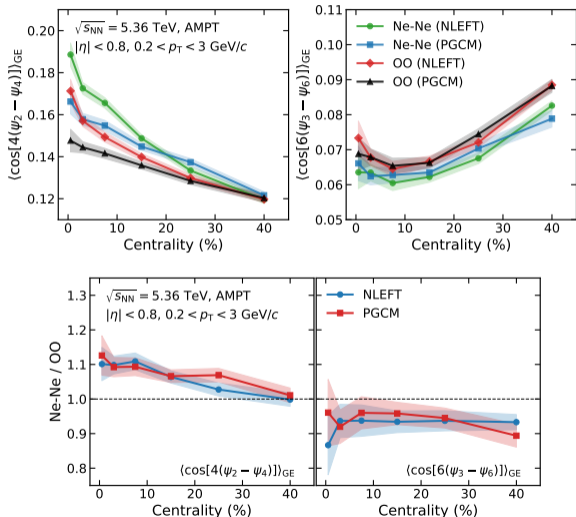
which is why GPUs become critical as k and combination count increase.

Example at $M = 3000$ (single combination, per event, relative units):

Order k	Naive M^k	vs $k = 2$	Q-vector kM
2	9.0×10^6	$1\times$	6.0×10^3
4	8.1×10^{13}	$9.0 \times 10^6\times$	1.2×10^4
6	7.29×10^{20}	$8.1 \times 10^{13}\times$	1.8×10^4

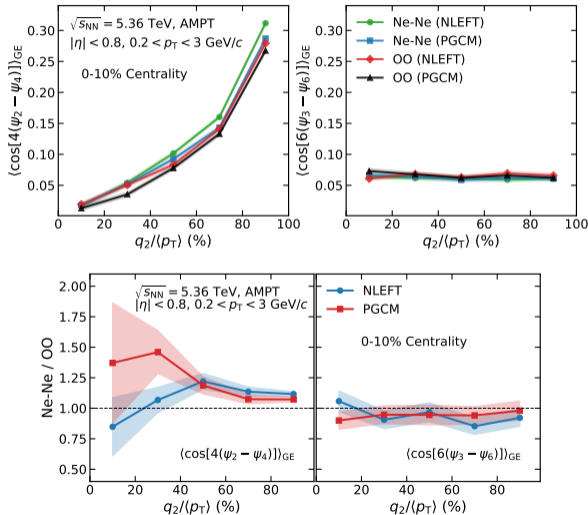
- AMPT is written in Fortran 77 and each executable run uses a single CPU core.
- One long serial run is inefficient for large statistics (millions of events).
- We use a bash workflow to split production into many independent jobs across cores.
- Each output file is then analyzed independently for each SPC observable in parallel.





- Centrality dependence of $\langle \cos[4(\Psi_2 - \Psi_4)] \rangle_{GE}$ and $\langle \cos[6(\Psi_3 - \Psi_6)] \rangle_{GE}$.
- Ne-Ne gives the larger $\langle \cos[4(\Psi_2 - \Psi_4)] \rangle_{GE}$, matching stronger quadrupole deformation.
- OO gives the larger $\langle \cos[6(\Psi_3 - \Psi_6)] \rangle_{GE}$, matching stronger triangular/octupole structure.
- The ratio highlights the clearest system split in central events, where intrinsic geometry survives best.

Prasad and Sahoo, arXiv:2605.00866 (2026).



- $q_2/\langle p_T \rangle$ is used to enrich tip-tip and body-body orientations.
- $\langle \cos[4(\Psi_2 - \Psi_4)] \rangle_{GE}$ rises toward body-body selections, reflecting stronger ellipticity-driven coupling.
- $\langle \cos[6(\Psi_3 - \Psi_6)] \rangle_{GE}$ changes much less, consistent with a more fluctuation-driven triangular component.
- The ratio confirms stronger Ne-Ne quadrupole sensitivity, while OO remains competitive for the triangular-sensitive correlator.

Prasad and Sahoo, arXiv:2605.00866 (2026).

- The two SPC observables show a clear and complementary sensitivity to nuclear geometry in light-ion collisions.
- $\langle \cos[4(\Psi_2 - \Psi_4)] \rangle_{GE}$ is larger in Ne–Ne, consistent with a stronger quadrupole-deformed initial geometry.
- $\langle \cos[6(\Psi_3 - \Psi_6)] \rangle_{GE}$ is larger in OO, consistent with a stronger triangular/octupole component.
- The Ne–Ne/OO ratios show that the strongest geometry discrimination appears in central events.
- Tip-tip/body-body selection mainly affects the elliptic-sensitive correlator, while the triangular-sensitive correlator remains much less orientation dependent.
- Together, these results support SPCs as robust probes of intrinsic nuclear structure, not only bulk collectivity.

Prasad and Sahoo, arXiv:2605.00866 (2026).

- AMPT provides a microscopic baseline with realistic non-equilibrium transport, rescattering, and finite-particle effects.
- The next step is a **hydrodynamic comparison** and additional higher order SPCs using the same OO and Ne–Ne nuclear configurations as initial conditions
- Hydro can test how much of the observed SPC pattern is controlled by:
 - initial-state geometry versus final-state response,
 - nonlinear mode couplings,
 - transport coefficients such as η/s and freeze-out choices.
- A useful program is: **NLEFT/PGCM geometry** → **hydro evolution** → **same GE-based SPC analysis**.
- If AMPT and hydro agree on the OO vs Ne–Ne SPC hierarchy, the case for geometry-driven signals becomes much stronger.

Heinz and Snellings, Ann. Rev. Nucl. Part. Sci. 63 (2013); Teaney and Yan, Phys. Rev. C 90 (2014); Gardim et al., Phys. Rev. C 85 (2012).

Thank You

for your attention

Suraj Prasad

HUN-REN Wigner Research Centre for Physics

suraj.prasad@wigner.hun-ren.hu

This work is supported by the Hungarian National Research, Development and Innovation Office (NKFIH) under the contract numbers NKFIH NKKP ADVANCED_25-153456, 2025-1.1.5-NEMZ_KI-2025-00005, 2024-1.2.5-TET-2024-00022, and the usage of Wigner Scientific Computing Laboratory (WSCLAB)

GPU Day 2026

- **Tip-tip collisions:** long axes of deformed nuclei align with the beam direction.
 - smaller transverse geometric eccentricity,
 - stronger radial push, typically larger $\langle p_T \rangle$.
- **Body-body collisions:** long axes lie in the transverse plane.
 - larger transverse eccentricity,
 - relatively weaker radial push.

Event-shape observables:

$$q_2 = \frac{1}{M} \left| \sum_{j=1}^M e^{2i\phi_j} \right|, \quad \langle p_T \rangle = \frac{1}{M} \sum_{i=1}^M p_{T,i}, \quad R \equiv \frac{q_2}{\langle p_T \rangle}.$$

- Higher R enriches body-body-like events (eccentricity dominates).
- Lower R enriches tip-tip-like events (radial flow dominates).